REPORT DOCUMENTATION PAGE

Form Approved
OMB NO. 0704-0188

1. AGENCY USE ONLY (Leave Blank)	2. REPORT DATE October 20, 2003	3. REPORT TYPE AND DATES COVERED FINAL, ~~12/15/00~~ 15 Apr 99 – 06/14/03
4. TITLE AND SUBTITLE STUDY OF THE PHYSICAL MECHANISMS OF ICE ADHESION		5. FUNDING NUMBERS DAAD19-99-1-0169
6. AUTHOR(S) Victor F. Petrenko		
7. PERFORMING ORGANIZATION NAME(S) AND ADDRESS(ES) Thayer School of Engineering, Dartmouth College HB 8000 Hanover NH 03755		8. PERFORMING ORGANIZATION REPORT NUMBER
9. SPONSORING / MONITORING AGENCY NAME(S) AND ADDRESS(ES) U. S. Army Research Office P.O. Box 12211 Research Triangle Park, NC 27709-2211		10. SPONSORING / MONITORING AGENCY REPORT NUMBER 39152.11-EV

11. SUPPLEMENTARY NOTES
The views, opinions and/or findings contained in this report are those of the author(s) and should not be construed as an official Department of the Army position, policy or decision, unless so designated by other documentation.

12 a. DISTRIBUTION / AVAILABILITY STATEMENT	12 b. DISTRIBUTION CODE
Approved for public release; distribution unlimited.	

In this research we have investigated main physical mechanisms of ice adhesion and developed several novel deicing and anti-icing methods. The following mechanisms of ice adhesion have been studied experimentally and theoretically:
1) electrostatic interactions between the electrical charge at the ice surface and the charge induced on a solid substrate;
2) hydrogen bonding between water molecules and substrate atoms; and
3) Liftshitz-van der Waals (LVW) dispersion forces.
Using that basic knowledge gained in the first part of the project we have invented, tested and developed the following deicing and anti-icing technologies:
1. Self-assembling mono-layer coating that drastically reduces adhesion of ice to metals.
2. Ice-electrolysis deicer.
3. High-frequency deicer.
4. Pulse electrothermal deicer.
5. Heat-storage deicer.
6. Lossy-dielectric deicer for high-voltage power lines.
7. HF-deicer for power lines.
We have also invented and developed three novel electrical methods capable to either decrease or increase friction on snow and ice. Five US and International patents were obtained and over 50 patent applications were submitted. One book and 15 scientific articles were published. The technologies were licensed to several US companies (9 licenses in total were issued The first airplane with our novel pulse deicer is scheduled to fly by the end of this year.

14. SUBJECT TERMS Ice, Ice Adhesion, Ice Surface, Deicing			15. NUMBER OF PAGES 37
			16. PRICE CODE
17. SECURITY CLASSIFICATION OR REPORT **UNCLASSIFIED**	18. SECURITY CLASSIFICATION ON THIS PAGE **UNCLASSIFIED**	19. SECURITY CLASSIFICATION OF ABSTRACT **UNCLASSIFIED**	20. LIMITATION OF ABSTRACT **UL**

REPORT DOCUMENTATION PAGE (SF298)
(Continuation Sheet)

List of manuscripts:

Book: Physics of Ice. Victor Petrenko and Robert Whitworth. Oxford University Press, 1999, 2001, 2003.

Journal Publications:

1. V. F. Petrenko and S. Qi: Effect of electric field on ice adhesion to stainless steel. Journal of Applied Physics, vol. 86, 5450-5454 (1999).

2.V. F. Petrenko: Methods and apparatus for modifying ice adhesion strength. World Intellectual Property Organization. PCT. International Publication Number WO 98/57851, 23 December 1998.

3. V. F. Petrenko and Z. Courville:. Active de-icing coating for aerofoils. Proceedings of AIAA-2000.

4. G. F. Bai, V. F. Petrenko, and I. Baker: "Study of dislocations in ZnS using electric force microscopy", MRS, Proc., v. 578, 255-260, 2000.

5. Z. Courville and V. F. Petrenko: De-icing layers of interdigitated microelectrodes. Materials Research Society, Symposium Proceedings, v. 604, 329-334, 2000.

6. S. Peng, V. F. Petrenko and M. Arakawa: Effect of self-assembling monolayers (SAMs) on ice adhesion to metals. Materials Research Society, Symposium Proceedings, v. 586, 261-266, 2000.

7. P. Donovan, V. F. Petrenko and M. Arakawa: Measurement of crack velocity in ice with high-speed photography, acoustic emission, and resistance method. Materials Research Society, Symposium Proceedings, v. 578, 321-326, 2000.

8. V. F. Petrenko and I. A. Ryzhkin: Violation of ice rules near surface: a new theory of quasi-liquid layer. Accepted for publication in Physical Review B, 2001.

9. Ryzhkin and V. F. Petrenko: Phase transition of an ice proton system into the Bernal-Fowler state. Physical Review B, v. 62 (17), 1-4, 2000.

10. G. F. Bai, V. F. Petrenko, and I. Baker: On the electrical properties of dislocations in ZnS using electric force microscopy. Will be published in May issue of Scanning. 2001.

11. Ryzhkin and V. F. Petrenko: Violations of ice rules near the surface: A theory for the quasiliquid layer, Phys. Rev. B., **65**, 012205, 2001.

12. Effect of Electric Fields on Friction Between Ice and Metals, Masahiko Arakawa, Victor F. Petrenko and Chen Cheng. Canadian Journal of Physics, v 81, 209-216, 2003.

13. Reduction of Ice Adhesion to Metal by Using Self-Assembling Monolayers (SAMs), V.F. Petrenko and S.Peng. . Canadian Journal of Physics, V 81, 387-393, 2003.

14. Observation of crack Ppropagation in saline ice and freshwater ice with fluid inclusion. Masahiko Arakawa[*1], Victor F. Petrenko[*2]. Canadian Journal of Physics, v81, 159-166, 2003.

15. Braking the ice. Charles Sullivan, Victor Petrenko, Joshua McCurdy and Valeri Kozliouk. IEEE Industry Applications Magazine, v9, No5, 49-54, 2003.

16. Pulse Electrothermal De-Icing, V. F. Petrenko, M. Higa, M. Starostin, and L. Deresh, Proceedings of The Thirteenth (2003) International Offshore and Polar Engineering Conference, Honolulu, Hawaii, USA, May 25030, 2003, pp. 435-438, 2003.

Scientific personnel supported:

1. Victor F. Petrenko, PI, Research Professor of Engineering.
2. Zoe Courville, PhD student
3. Gabriel Martinez, MS student
4. Taylor Smith, undergraduate student
5. Michiya Higa, research associate

Report of Inventions
Patents:

1. Systems and Method for modifying Ice Adhesion Strength. United States Patent #6,027,075, Feb 22, 2000.
2. Systems and Method for modifying Ice Adhesion Strength. United States Patent #6,427,946 B1, Aug 6, 2002.
3. Systems and Method for modifying Ice Adhesion Strength. United States Patent #6,563,053 B2, May 13,2003.
4. Reduction of Ice Adhesion to Land Surfaces by Electrolysis", United State Patent #6,576,115, June 10, 2003.
5. Systems and Method for modifying Ice Adhesion Strength. Chinese Patent #ZL 98806257.7, Jan 2, 2002.
6. Systems and Method for modifying Ice Adhesion Strength. Chinese Patent #ZL 15095.9, April 23, 2003.
7. 38 pending patent applications on de-icing of roadways, power lines, planes, roofs, windshield, sea ships, ice prevention, ice and snow friction control.

Table of Contents

Study of The Physical Mechanisms of Ice Adhesion

PI: Victor F. Petrenko
Thayer School of Engineering, Dartmouth College, Hanover, NH 03755

1. Abstract

In this research we have investigated main physical mechanisms of ice adhesion and have developed several novel deicing and anti-icing methods. The following mechanisms of ice adhesion have been studied experimentally and theoretically:

1) electrostatic interactions between the electrical charge at the ice surface and the charge induced on a solid substrate;
2) hydrogen bonding between water molecules and substrate atoms; and
3) Liftshitz-van der Waals (LVW) dispersion forces.

Using that basic knowledge gained in the first part of the project we have invented, tested and developed the following deicing and anti-icing technologies:

1. Self-assembling mono-layer coating that drastically reduces adhesion of ice to metals.
2. Ice-electrolysis deicer.
3. High-frequency deicer.
4. Pulse electrothermal deicer.
5. Heat-storage deicer.
6. Lossy-dielectric deicer for high-voltage power lines.
7. HF-deicier for power lines.

We have also invented and developed three novel electrical methods capable to either decrease or increase friction on snow and ice.

Five US and International patents were obtained and over 50 patent applications were submitted. One book and 15 scientific articles were published. The technologies were licensed to several US companies (9 licenses in total were issued). The first airplane with our novel pulse deicer is scheduled to fly by the end of this year.

2. Formal results:

2.1 List of manuscripts:

Book: Physics of Ice. Victor Petrenko and Robert Whitworth. Oxford University Press, 1999, 2001, 2003.

Journal Publications:

1. V. F. Petrenko and S. Qi: Effect of electric field on ice adhesion to stainless steel. Journal of Applied Physics, vol. 86, 5450-5454 (1999).
2. V. F. Petrenko: Methods and apparatus for modifying ice adhesion strength. World Intellectual Property Organization. PCT. International Publication Number WO 98/57851, 23 December 1998.
3. V. F. Petrenko and Z. Courville:. Active de-icing coating for aerofoils. Proceedings of AIAA-2000.
4. G. F. Bai, V. F. Petrenko, and I. Baker: "Study of dislocations in ZnS using electric force microscopy", MRS, Proc., v. 578, 255-260, 2000.
5. Z. Courville and V. F. Petrenko: De-icing layers of interdigitated microelectrodes. Materials Research Society, Symposium Proceedings, v. 604, 329-334, 2000.
6. S. Peng, V. F. Petrenko and M. Arakawa: Effect of self-assembling monolayers (SAMs) on ice adhesion to metals. Materials Research Society, Symposium Proceedings, v. 586, 261-266, 2000.
6. P. Donovan, V. F. Petrenko and M. Arakawa: Measurement of crack velocity in ice with high-speed photography, acoustic emission, and resistance method. Materials Research Society, Symposium Proceedings, v. 578, 321-326, 2000.
7. V. F. Petrenko and I. A. Ryzhkin: Violation of ice rules near surface: a new theory of quasi-liquid layer. Accepted for publication in Physical Review B, 2001.
8. Ryzhkin and V. F. Petrenko: Phase transition of an ice proton system into the Bernal-Fowler state. Physical Review B, 62 (17), 1-4, 2000.
9. G. F. Bai, V. F. Petrenko, and I. Baker: On the electrical properties of dislocations in ZnS using electric force microscopy. Will be published in May issue of Scanning. 2001.
10. Ryzhkin and V. F. Petrenko: Violations of ice rules near the surface: A theory for the quasiliquid layer, Phys. Rev. B., 65, 012205, 2001.
11. Effect of Electric Fields on Friction Between Ice and Metals, Masahiko Arakawa, Victor F. Petrenko and Chen Cheng. Canadian Journal of Physics, v 81, 209-216, 2003.
12. Reduction of Ice Adhesion to Metal by Using Self-Assembling Monolayers (SAMs), V.F. Petrenko and S.Peng. . Canadian Journal of Physics, V 81, 387-393, 2003.
13. Observation of crack Ppropagation in saline ice and freshwater ice with fluid inclusion. Masahiko Arakawa*1, Victor F. Petrenko*2. Canadian Journal of Physics, v81, 159-166, 2003.
14. Braking the ice. Charles Sullivan, Victor Petrenko, Joshua McCurdy and Valeri Kozliouk. IEEE Industry Applications Magazine, v9, No5, 49-54, 2003.

15. Pulse Electrothermal De-Icing, V. F. Petrenko, M. Higa, M. Starostin, and L. Deresh, Proceedings of The Thirteenth (2003) International Offshore and Polar Engineering Conference, Honolulu, Hawaii, USA, May 25030, 2003, pp. 435-438, 2003.

2.2 Report of Inventions
Patents:

1. Systems and Method for modifying Ice Adhesion Strength. United States Patent #6,027,075, Feb 22, 2000.
2. Systems and Method for modifying Ice Adhesion Strength. United States Patent #6,427,946 B1, Aug 6, 2002.
3. Systems and Method for modifying Ice Adhesion Strength. United States Patent #6,563,053 B2, May 13,2003.
4. Reduction of Ice Adhesion to Land Surfaces by Electrolysis", United State Patent #6,576,115, June 10, 2003.
5. Systems and Method for modifying Ice Adhesion Strength. Chinese Patent #ZL 98806257.7, Jan 2, 2002.
6. Systems and Method for modifying Ice Adhesion Strength. Chinese Patent #ZL 15095.9, April 23, 2003.

38 pending patent applications on de-icing of roadways, power lines, planes, roofs, windshield, sea ships, ice prevention, ice and snow friction control.

3. Main Accomplishments:

3.1 Active de-icing coating for aerofoils

We developed a special active coating that is capable to de-ice various solid surfaces vulnerable to icing such as airplane wings, helicopter blades, road signs, superstructures and hulls of ships *etc*. The coating consist of a thin web of metal interdigitated micro-electrodes formed using photolithography. The electrodes are made of very thin (5 micrometer) copper-clad or titanium-clad laminate on thin and flexible kapton substrate, see figure 1. Typical inter-electrode spacing and electrode width varied from 10 to 100 micrometers. After etching the electrodes were electroplated with Pt to increase their resistance to electro-corrosion. The de-icing action of the coating is based on the phenomenon of ice electrolysis. Namely, when ice is growing over electrodes a small DC bias of 5 V to 25 V is applied to the electrodes generates DC current through the ice. The ice adjacent to the electrodes then decomposed in gaseous hydrogen (on the cathode) and gaseous oxygen (on the anode) thus eliminating bonding between the ice and the metal.

Moreover, gas bubbles rapidly growing on the interface spread as interfacial cracks thus breaking ice, figure 2. We also developed a theory of such active grids. We also demonstrate a video record of de-icing action of the coating. Figure 3 shows a dramatic decrease in the ice adhesion strength when the DC voltage was applied to the grid elelctrodes.

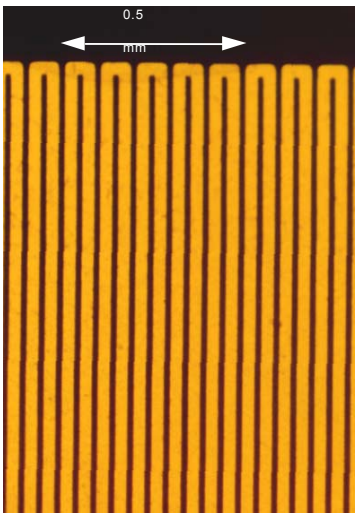

Figure 1. Electroplated copper grid electrodes on 125 μm kapton film. The gold-plated copper electrodes appear black.

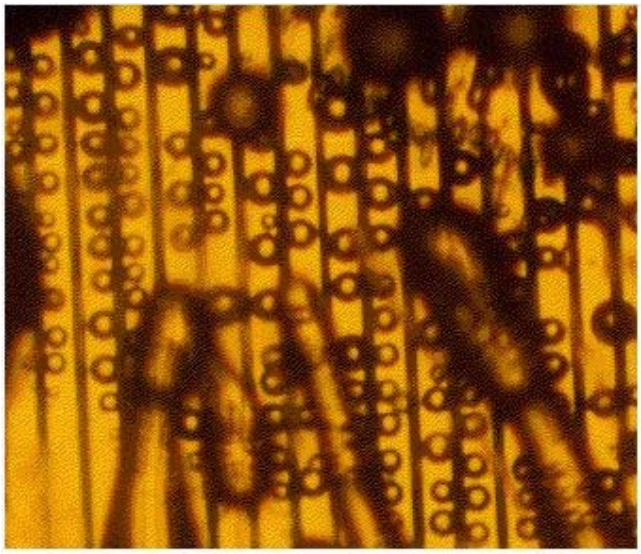

Figure 2. Initial stage of bubble generation on a gold grid in ice as seen 10 s after 6 volts was applied. T = –10˚C. The small circular bubbles were generated on the interface by ice electrolysis. The large gas bubbles of odd shapes were formed in the ice bulk during freezing.

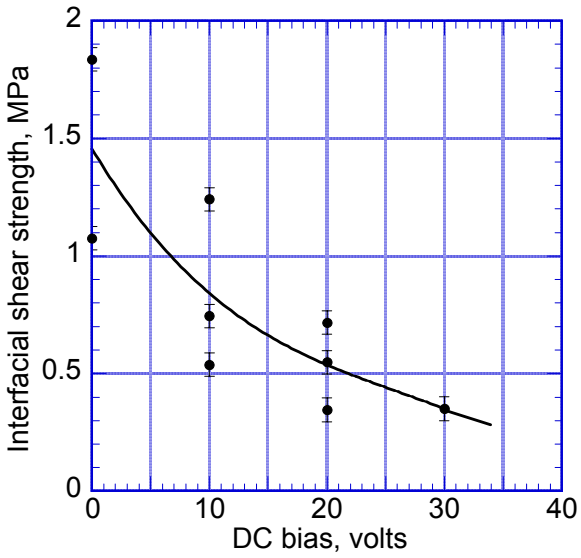

Figure 3. Dependence of shear strength of the ice/grid interface on voltage applied after the ice was formed. Pre-applied voltage was 5 V. T = -8˚C.

3.2 Effect of self-assembling monolayers on ice adhesion to metals

Strong adhesion of ice to almost all known solids is a serious engineering problem that has not been solved yet because physical mechanisms of ice adhesion are not understood. In this research we used an original method to study the role of hydrogen bonding in ice adhesion and to minimize the effect of this mechanism on ice adhesion. For this purpose, we coated metals (Au and Pt) with a mono-molecular layers of specific organic molecules that had either strong hydrophobic properties (CH3(CH2)11SH) or strong hydrophilic properties (OH3(CH2)11SH), see figure 4. To determine the contribution of hydrogen bonding to ice adhesion SAMs of varying hydrophobia/hydrophilia were made by mixing the hydrophobic and hydrophilic components. All the films were built of similar molecules that differed only in their outermost groups, OH- and CH3. Thus, when the films were grown on the same substrate (almost atomically smooth metal films) any difference in their adhesion to ice were due to the difference in the hydrogen bonding between the ice and SAM's. The films' structure and quality were examined with SPM and the degree of SAM's hydrophobia/hydrophilia was characterize with a contact angle of water on the films. We have then frozen water on the films and measured shear strength of ice/SAM/metal interfaces. Possible damage to the interfaces was examined with SPM after the ice was melted. We found a strong correlation between the degree of hydrogen bonding and the ice adhesion strength, figure 5. Though, the hydrogen bonding was found neither single nor major mechanism contributing in ice adhesion.

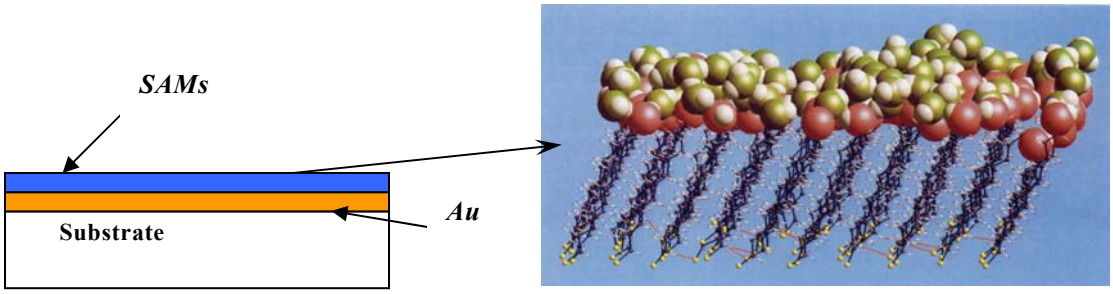

Figure 4. A schematic diagram showing the structure of SAMs bound to the gold surface.

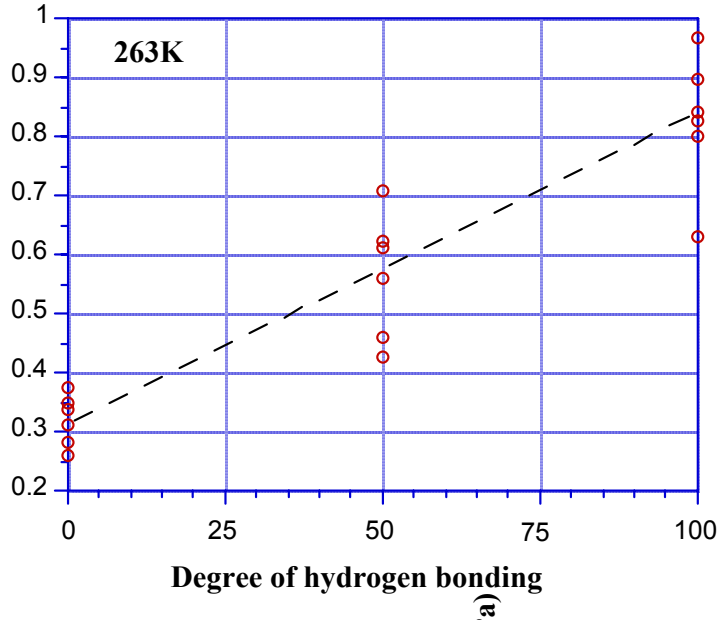

Figure 5. Effect of degree of hydrogen bonding on the ice/SAM shear strength**.**

3.3 Theoretical Results:

3.3.1 Phase transition of an ice proton system into Bernal-Fowler state

We developed a new microscopic model of an ice proton system. A mean field approximation was used to study disorder-partial order transition in the proton subsystem of ice. This analysis revealed that ice rules arise as a result of the second order phase transition. From the theoretical point of view, above the phase transition temperature the protons should be distributed over all possible positions without any restrictions. However, in real ice under zero pressure the disordering of the proton lattice apparently leads to ice melting. We also derived the Landau-Ginzburg equation suitable for the model under consideration and showed that the theories based on ice rules must be modified when one is working in the region of the critical temperature.

3.3.2 Violation of ice rules near the surface: a new theory for the quasi-liquid layer

We propose a new theoretical model of a quasi-liquid layer on the ice surface. Our model is based on the recently proposed theory of the transition of ice into the Bernal-Fowler state [1] and does not need any additional assumption. In our model, unique properties of ice near the surface arise from a reduction in an order parameter due to a specific boundary condition on the ice surface. The theory may be directly generalized to the ice/solid interfaces.

3.4. Freezing Point Depression

We discovered a new physical phenomenon: depression of water freezing point under action of electric field. In our preliminary tests, conducted with interdigitated gold electrodes, we found that when a weak direct current $j \geq 1$ mA/cm2 passes through pure water, the layer directly adjacent to the electrode does not freeze, even at T = –10°C. When the voltage (5 V) was not applied the water froze down to the electrodes. Application of the voltage after freezing did not cause melting of the pre-electrode layer of ice. The thickness of the unfrozen layer was estimated optically as 5 to 25 □m in various locations on the grid.

This effect cannot be due to electric heating for the following reasons. The temperature of the substrate and the ice above the layer, as measured with a thin thermocouple, was maintained at –10°C and a simple estimate showed that the low electric power per cm2 dissipated in those experiments (≤ 5 mW/cm2) could warm the unfrozen layer by only 0.05°C. The existence of this unfrozen layer dramatically decreases the shear strength of the ice/substrate interface and, thus, is critically important.

We are going to study this intriguing phenomenon thoroughly. Our working hypothesis is that the direct current causes an injection of intrinsic ions into the water, thus depressing the freezing point. We found earlier that even a weaker direct current (100 A/cm2) that passes through pure water changes the electrical conductivity of thin pre-electrode layers of pure water by orders of magnitude.

This phenomenon is fully reversible and water regains its physical properties within about 10 seconds after the DC bias is shut off. The maximum effect was observed very close to the electrodes.

In a series of other tests we have studied this phenomenon experimenting with aluminum/alumina/platinum electrode assembly shown in figure 6.

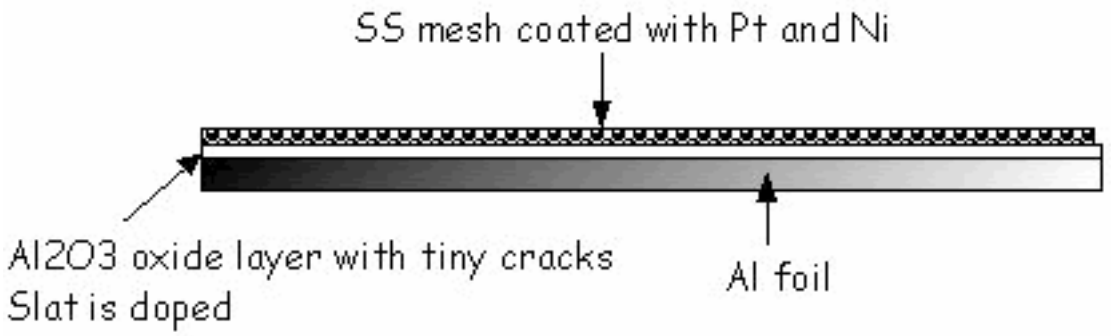

Figure 6. Electrode assembly used in the freezing-point depression experiments. The aluminum foil is used as a cathode, porous Al2O3 film (10-μm thick) is used as an insulating layer, and stainless steel mesh electroplated with nickel and platinum is used as an anode. 400-gauge mesh woven of 22.4 μm wire was used.

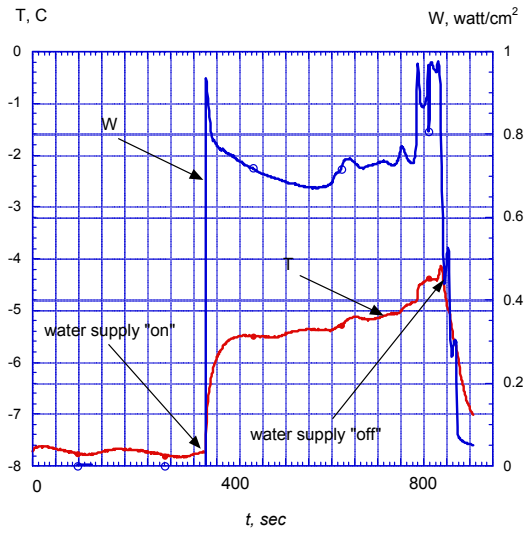

Figure 7. Record of the leading-edge temperature and electric power dissipated in the mesh electrodes (figure 2) in a wind-tunnel experiment. Air speed v = 200 mile/h, air temperature T_{air} = -12C, water content c = 0.25g/m3.

The aluminum foil was stretch over a massive aluminum aerofoil cooled either with circulating liquid coolant or with high-speed (200 mile/hour) cold air in a wind tunnel. Two thin thermocouples were inserted in the aluminum cylinder at 2 mm and 25 mm from the mesh. An example of wind-tunnel test results can be seen in figure 7. Even without electric power applied to the mesh the mesh temperature exceeded the ambient air temperature due to adiabatic compression of the air at the leading edge of the aerofoil. With the power applied that temperature rises but remains well below the water freezing point.

Nevertheless, in that experiment ice has not formed and the on the mesh has remained liquid.

One possible mechanism of the effect is injection of H_+ and OH_- ions from the interfaces into the water. The ions are generated on the electrodes according to the reactions:

$$2H2O + 2e_- \Leftrightarrow 2H_\bullet + 2OH_- \quad (1)$$

and

$$2H2O - 2e_- \Leftrightarrow O_\bullet + 2H_+ \text{ (anode)} \quad (2)$$

where $O_\bullet$ and $H_\bullet$ are atomic oxygen and hydrogen.

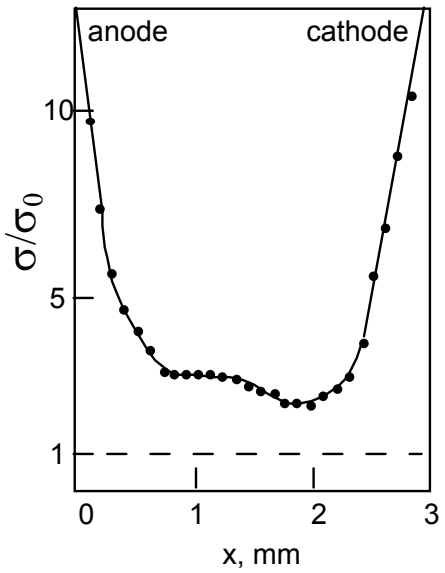

Figure 8. Relative increase in conductivity of distilled water placed between two pt electrodes. ac conductivity was measured at f = 1 kHz. the applied DC bias was 5 v. t = 20˚C. initial conductivity of water $\sigma = 10^{-3}$ s/m.

Additional ions are generated when those atoms recombine into molecules of oxygen and hydrogen. Each recombination event releases about 5 eV of energy, and that energy is sufficient to break several neighboring water molecules into H_+ and OH_- ions.

We estimated that as many as 10% of the water molecules near the electrodes may dissociate into ions; this is equivalent to an H_+ or OH_- concentration of 3.08 mol. Without exclusions, dissolution of ions in water results in depression of the freezing point. Thus, an NaCl solution of 3.08 mol has a freezing-point depression of –11.25°C. By doping water with KOH (OH_- and K_+ ions), the freezing point can be lowered to –63°C (at 20 molecular % of KOH).

A thermodynamic reason for the freezing point depression is that dissolution of ions in such a highly polar liquid as water lowers the free energy of the water. These ions affect the free energy of ice to a much lesser degree, due to the fact that the microscopic dielectric constant of ice is just 3.2, while in water it equals 87 (at 0°C). Also, impurity ions are much less soluble in ice than in water. Thus, ions decrease the free energy of water but leave that of ice almost unchanged. Because of this, the free energy of water remains less than that of ice down to lower temperatures, thus delaying the phase transition.

The basic objective of this part of the research will be to understand the mechanism responsible for the freezing-point depression observed in near-electrode layers of water. We will examine the hypotheses that: (1) the effect is due to electrolysis of water and formation of atomic H and O on the metal/water interfaces, which leads to the production of H^+ and OH^- ions; (2) the effect is due to electrolysis of water and the production of H^+ and OH^- ions directly on the metal/water interface; and (3) the effect is due to an enthalpy change (heat production).

3.5 Plasma-coating de-icer for power lines

A plasma anti-icing coating is a shell that encloses a thin layer of air around each transmission wire. When ice accretes on the shell, the ice molecules polarize in the 60-Hz electric field and increase the electric charge on the shell's surface. This additional charge increases the electric field strength inside the thin air layer and causes corona discharges; in other words, the air breaks down into a hot ionized gas, or plasma. The geometry of the shell and the thickness of the air layer can be used to adjust the corona threshold so heating begins exactly when ice of a predetermined thickness forms. This automatic and ice-sensitive on/off mechanism demonstrates the elegance of the plasma coating method.

Theoretical estimates are developed on the following pages, showing that a plasma coating can generate approximately three-times the heating power of a dielectric coating, for the same coating thickness. High heating power is a performance advantage that can enable the plasma coating to prevent icing in the most demanding conditions, such as high winds and cold temperatures; or if heating power is unnecessarily high, it can be reduced to minimize manufacturing costs and material usage. An example of a plasma coating configuration that sacrifices heating power for increased heat dissipation from the conductor and manufacturability, is a porous, closed-cell, foam plastic. There is wide flexibility to choose materials for desirable mechanical properties and high resistance to weathering because, unlike the dielectric coating, the plasma coating’s shell does not require specific electrical properties.

We give a brief explanation of the theory of plasma coatings and the tests that we performed using small prototypes. Further research, materials testing, and testing on energized lines is necessary to optimize the method, but it has undeniable potential for economical icing protection because of its high heating power and flexibility for materials.

Diagrams of several possible plasma coating configurations are shown here, but a more complete discussion of performance tradeoffs, potential effects on transmission efficiency, and manufacturing considerations is given in the supplementary report, "Anti-Icing Coating Development Strategy." Prospective manufacturing partners are discussed and listed in "Prospective Industrial Partners for Full-Scale Development of Anti-Icing Cables: Interwire 2001 Exposition."

More Explanations of the Plasma Coating Method.

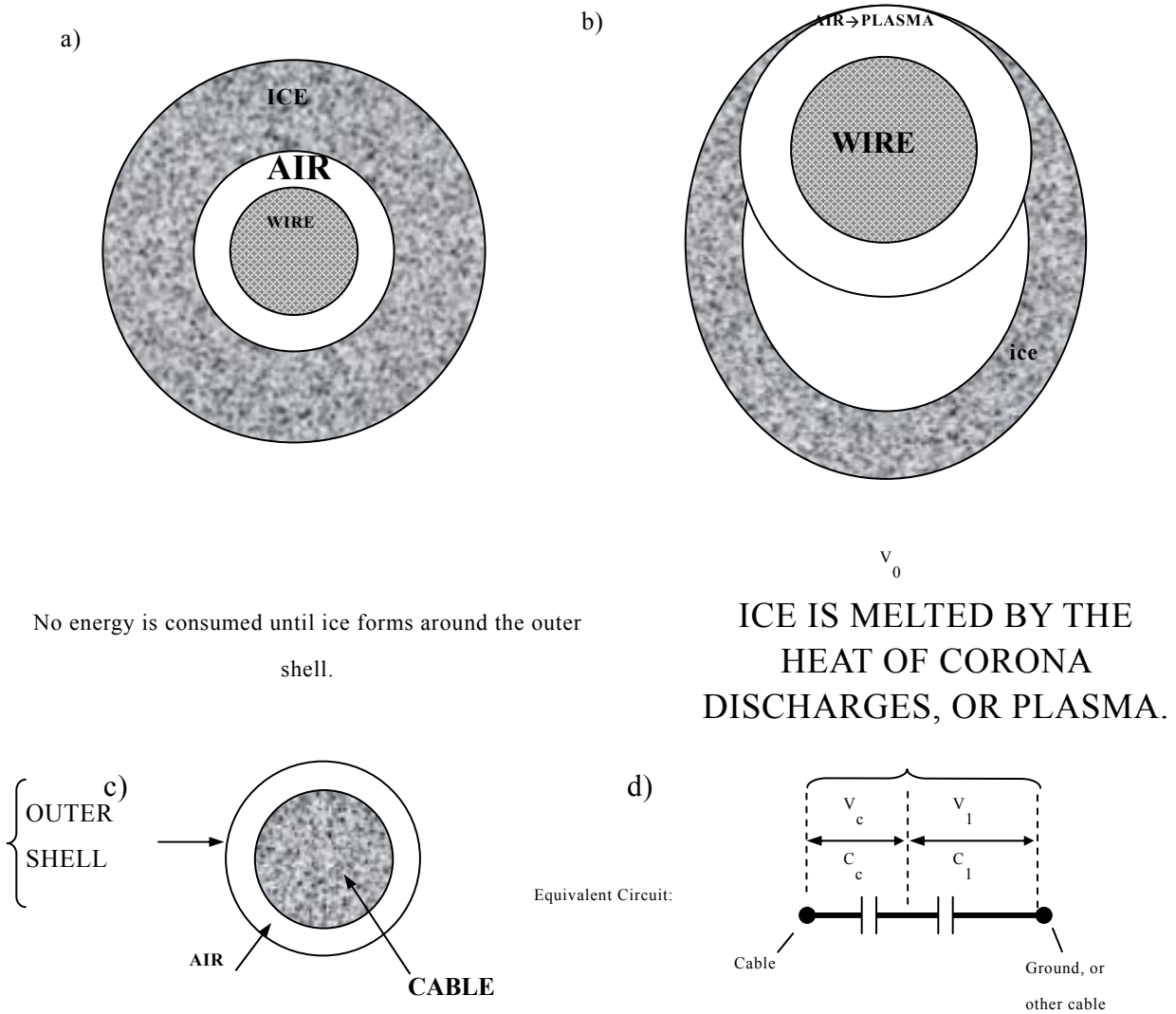

Figure 9. Schematics of the plasma-coating method. V_0 is the line voltage.C_c is a capacitance of the air layer between the central cable and the outer shell. C_1 is the total earth and interwire capacitance.

a)

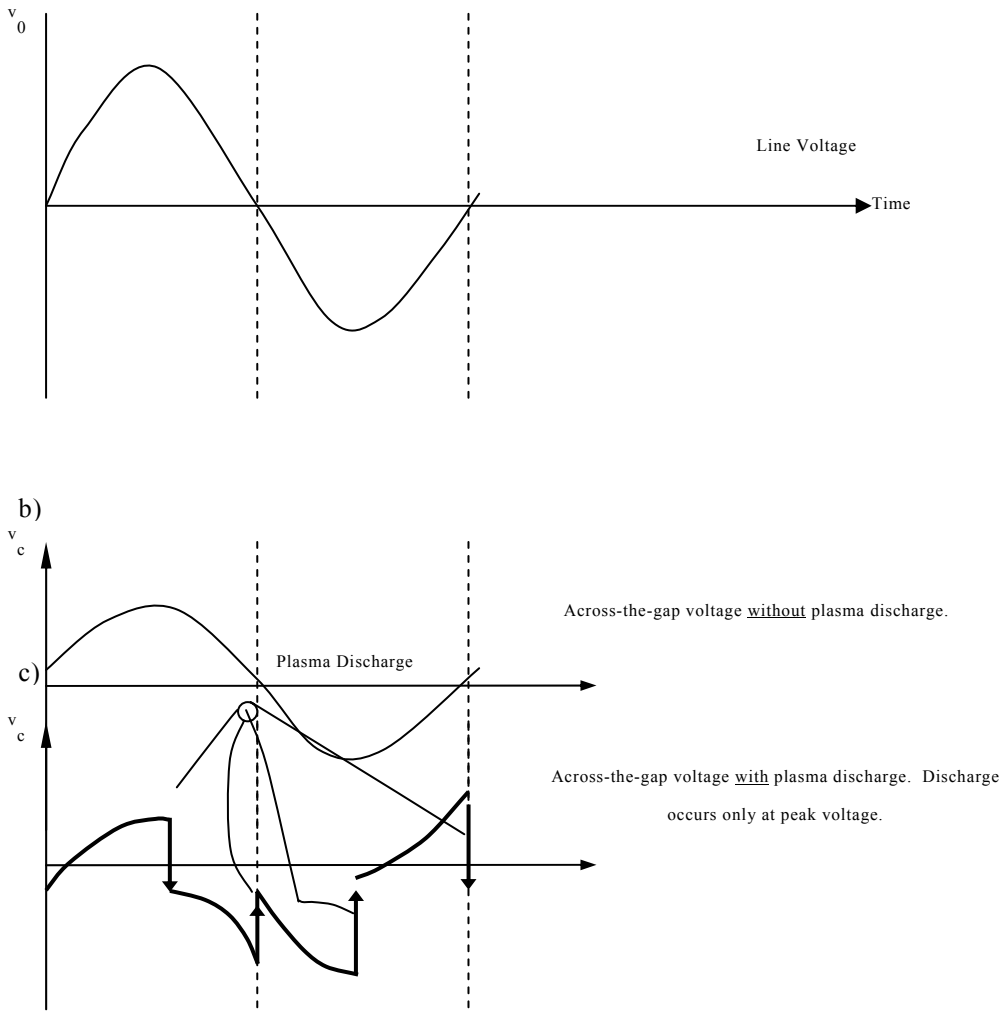

Figure 10 illustrates how the circuit works.Figure 10b shows the voltage, V_c, across the coating gap capacitance C_c, without ice. There are no discharges in 10b because V_c is below the corona threshold. However, the presence of ice causes the transmission line to charge C_c past the corona threshold, shown in Figure 10c. This coating capacitance C_c is discharged four times per cycle of AC, as shown in the diagram Figure 10c; each time, the total charge on Cc is returned to the transmission line.

When fully charged, the electric energy stored in the gap capacitor C_c is:

$$\frac{C_c V_c^2}{2}, \text{ where } V_c^2 \text{ is a peak (not rms) value.} \quad (3)$$

With an rms voltage V'_G the energy is: $C_C\left(V'_C\right)^2$. For a transmission line frequency *f*, there are 4*f* such discharges per second. The total electric power dissipated is:

$$W_h^* = 4f\, C_C\left(V'_C\right)^2 = \frac{4f\, C_1^2\, V_0^2}{C_1 + C_C} \qquad (4)$$

where V0 is the rms line voltage. That heating power significantly exceeds the maximum heating power of a dielectric coating, where ε is a dielectric constant of the solid coating:

$$W_h = \frac{\omega\, C_1^2\, V_0^2}{2\left(C_1 + \varepsilon C_C\right)} \qquad (5)$$

Because CC>>C1, even for the best solid coating (ε=2.3) $\frac{W_h^*}{W_h} \approx 3$. (6)

In practice, there can be thousands of discharges per cycle if the outer shell is made from an insulating material, such as plastic or glass. The total charge on the shell is discharged only four times per cycle, as shown in the calculations above, but this can occur in many local discharges. This type of evenly distributed, local discharges, or a continuous glow discharge, will cause insulating shells to heat more evenly and reliably than metal, or electrically conductive, shells. Corona discharges inside of metal shells are more likely to take the form of large sparks, concentrating heating power at a few isolated locations and corroding the shell.

3.6 High-frequency dielectric-heat de-icing of engineering structures

A new method of ice protection and ice prevention was invented, theoretically calculated and tested in cold rooms and a new wind-tunnel of Thayer School of Engineering. The new method is based on high-frequency heating and evaporation of interfacial ice. The method uses the same types of electrodes that are used in the electrolysis method: interdigitated circuits, woven meshes, laminate structures, etc. But the electrodes are not under electrocorrosion attacks. Because of this, a choice of electrode material is much wider.

The method utilizes the fact that ice conductivity at high frequencies is much higher than that for DC and low frequency. Moreover, conductivity of free ice surface and ice/solid interfaces also exceeds bulk conductivity. As a result, when low-voltage high-frequency electric power is applied to ice/solid interface it can easily melt and even evaporate the interfacial ice, thus braking ice/substrates bonds. Because of very low DC- and low-frequency conductivity of ice, it is usually not possible to melt ice by applying such electric power. Normally, electric breakdown of ice and air occurs before the ice can

be melted. However, at frequencies above Debye frequency *f*D ice conductivity rises by two to three orders of magnitude making electric melting possible.

In comparison with conventional heaters our new method has two main advantages:

1. Interfacial ice can be melted without heating any part of protected structure over 0°C. That drastically reduces the heat exchange with environment and thus reduces power required for de-icing.
2. The HF-heating power is focused on a very thin (5 μm to 50 μm-thick) layer of interfacial ice and, thus, the power is used more rationally, see figures 11-12. That too decreases the total power consumed by the device.

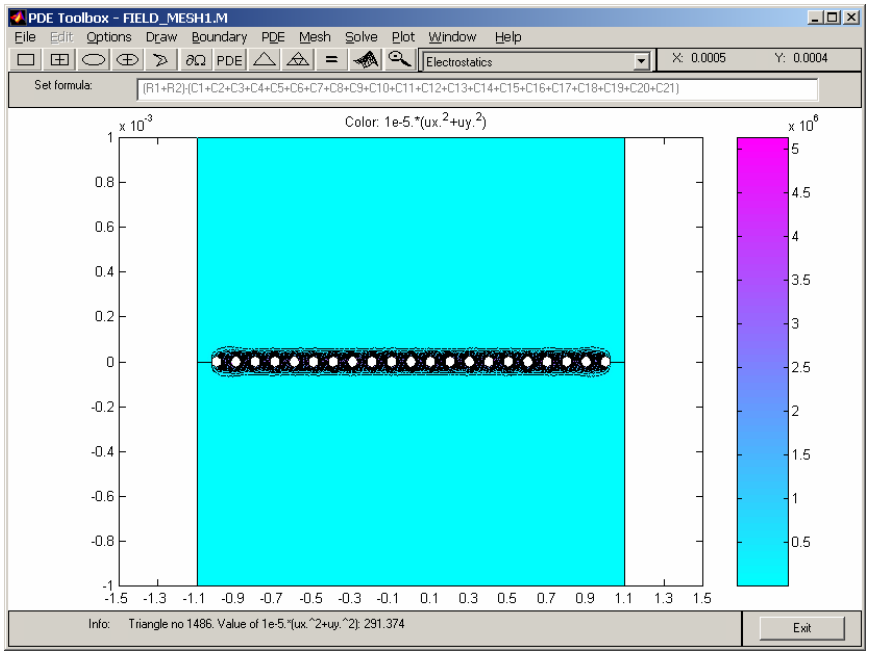

Figure 11 MatLab modeling of density of heating power generated by HF electric field in ice. Mesh wires are 50 μm in diameter, mesh pitch is 100 μm. 30V is applied between neighboring wires. Contours show lines of equal power. It is seen that heat is generated within an ice layer of about 50 μm thick.

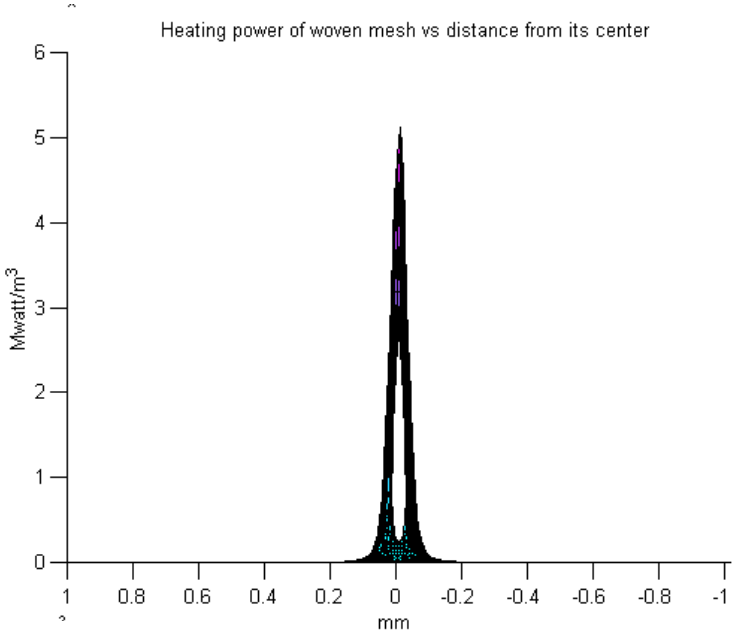

Figure 12. Heating power for the same as in Figure 4 mesh as a function of a distance from the mesh center.

The frequency should be above the Debye frequency that depends on temperature and ice purity. In pure ice Debye frequency changes from 1 kHz at -20°C to about 30 kHz at 0°C. One remarkable thing about a high-frequency de-icer is that it also can prevent ice formation, as it's described below.

3.7 Ice Prevention Experiments.

Operating and geometrical parameters for such HF-de-icer were theoretically calculated, and dozens of de-icers were tested in a temperature range from -5°C to -30°C and a wind velocity up to 320 km/h. Details of the theory of operation and several examples of HF de-icer are given in Appendix II.

A de-icer for anti-icing action was made of aluminum foil as first electrode, 10-μm thick anodized aluminum as an insulating layer, and a thin 400-gauge SS mesh woven of 25 μm wires. The sample has dimensions of 50mmx50mm. 5-mm thick ice was grown on the sample surface and AC power at 20 kHz was then applied. Figure 5 shows heating power versus voltage dependence recorded in that experiment. As it seen from the figure, the heating is was below 50 volts and than jumped to 4.7 kwatt/m2 when ice on the interface was melted. That occurred because water conductivity exceeds that of ice by two orders of magnitude. Notice, that reduction of the power down to 300 watt/m2 left the interface unfrozen. This is what we call "Anti-Icing" action. Only below that threshold of the "freezing point depression" the water froze.

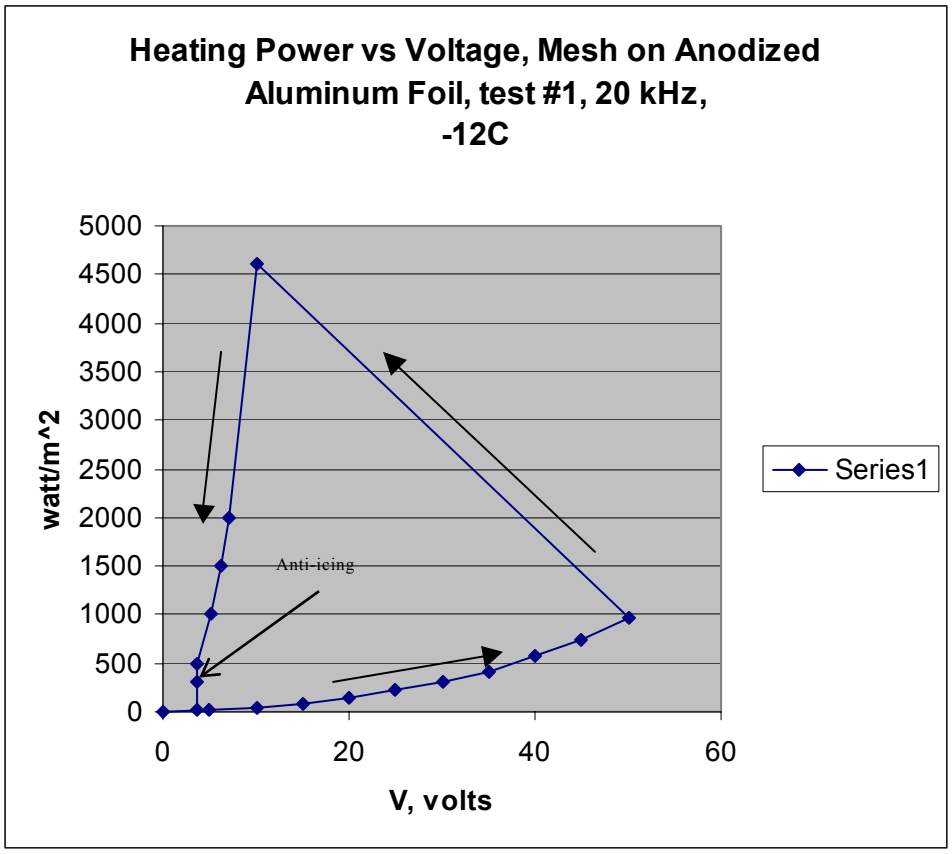

Figure 13. Record of electric power versus voltage for HF de-icer. The arrows indicate the sequence in which the voltage was applied.

In real environment there is always some wind that can change significantly heat exchange between a de-icer and environment. To take this effect into account, we perform many experiments in a new wind-tunnel of Thayer School of Engineering.

3.7.1 Theoretical background: Heating Power and Heat Transfers of a Coil-based HF-de-icer

Let us consider a de-icer made of a bifiler wound coil:

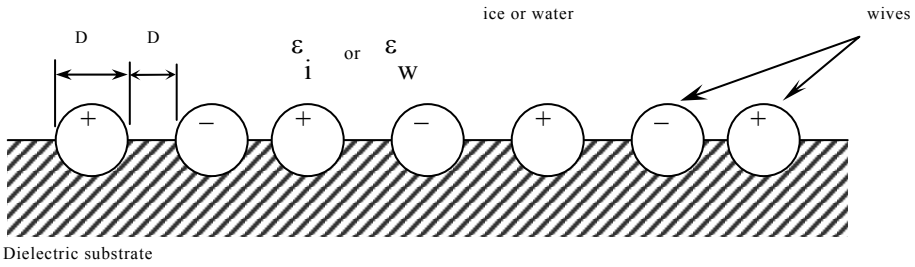

Figure 14 Cross section of a coil-based HF de-icer

Computer modeling (PDE Toolbox of MatLab) shows that at high frequencies ($f \geq 10k\ Hz$) the ice-related capacitance Ci and ice-related conductance Gi per one square meter are:

$$C_i \cong \frac{1.2 \cdot 10^{-11}}{D(m)} \cdot \frac{F}{m^2} \tag{7}$$

$$G_i = \frac{0.53 \cdot 10^{-4}}{D(m)} \cdot \mathrm{e}^{6670\left(\frac{1}{273} - \frac{1}{T(k)}\right)} \left(\frac{1}{\mathrm{ohm} \cdot m^2}\right) \tag{8}$$

where D is given in meters and T in Kelvin's.

The same modeling showed that electric breakdown of air occurs at voltage VB:

$$V_B = 2.4 \cdot 10^6 \cdot D(m) \tag{9}$$

Equation (3) implies that at sea level the air-breakdown electric field is 30kV/cm. In terms of rms:

$$V_B \approx 1.7 \cdot 10^6\, D(m) \tag{10}$$

To keep the voltage below safe level, let us keep it at 70% of what eqn. (9) shows.

$$V_B = 1.2 \cdot 10^6 D(m) \;=\; V_{\max} \tag{11}$$

Then, combining eqns. 8 & 11, we can find the maximum heating power:

$$W_{\max}(T) = G_i V_{\max}^2 = 0.763 \cdot 10^8 \cdot D(m) \cdot \mathrm{e}^{6670\left(\frac{1}{273} - \frac{1}{T}\right)} \tag{12}$$

For an arbitrary voltage V, the power is:

$$W(T,V) = W_{\max}(T) \cdot \left(\frac{V}{V_{\max}}\right)^2 \tag{13}$$

In Appendix A I showed that using 0.5mm wires and "safe" voltage of 600 volts (rms). We will need 13 seconds to melt the interface at -30°C, 4.3 seconds to melt the interface at -20°C and just 1.2 seconds at -10°C. Ice growth rate usually does not exceed 1.5mm/min.

Thus, if we shed ice every two minutes, as shown in the Appendix A, it would take approximately average power of:

$$\begin{cases} 1.75 \text{ kW/m2} & \text{at- } 30°C \\ 1 \text{ kW/m2} \quad \text{at} & \text{- } 30°C \\ 0.47 \text{ kW/m2} & \text{at- } 30°C \end{cases}$$

Let us now add the power it takes to keep 5mm-wide parting strip on stagnation line free of ice. Power density: 40 kw/m2, 4-inch wide protected band:

$$P_a^1 = 40\frac{kW}{m^2} \cdot \frac{1}{5} inch \frac{1}{4\ inch} = 2kW/m^2$$

Then, even at -30°C the total power consumption:

$$1.75 + 2 = 3.75\frac{kW}{m^2} \quad \leq 10\% \text{ of conventional DC heater}$$

If we figure out how to break mechanically 3-mm thick ice on the stagnation line, we can use $1\frac{kW}{m^2}$ in most cases.

3.7.2 HF-windshield de-icer

The HF-de-icing method that was described above has been adjusted for use on transparent surfaces such as car windshields and building windows.

The following HF-deicer samples were made and tested:

Draw of sample

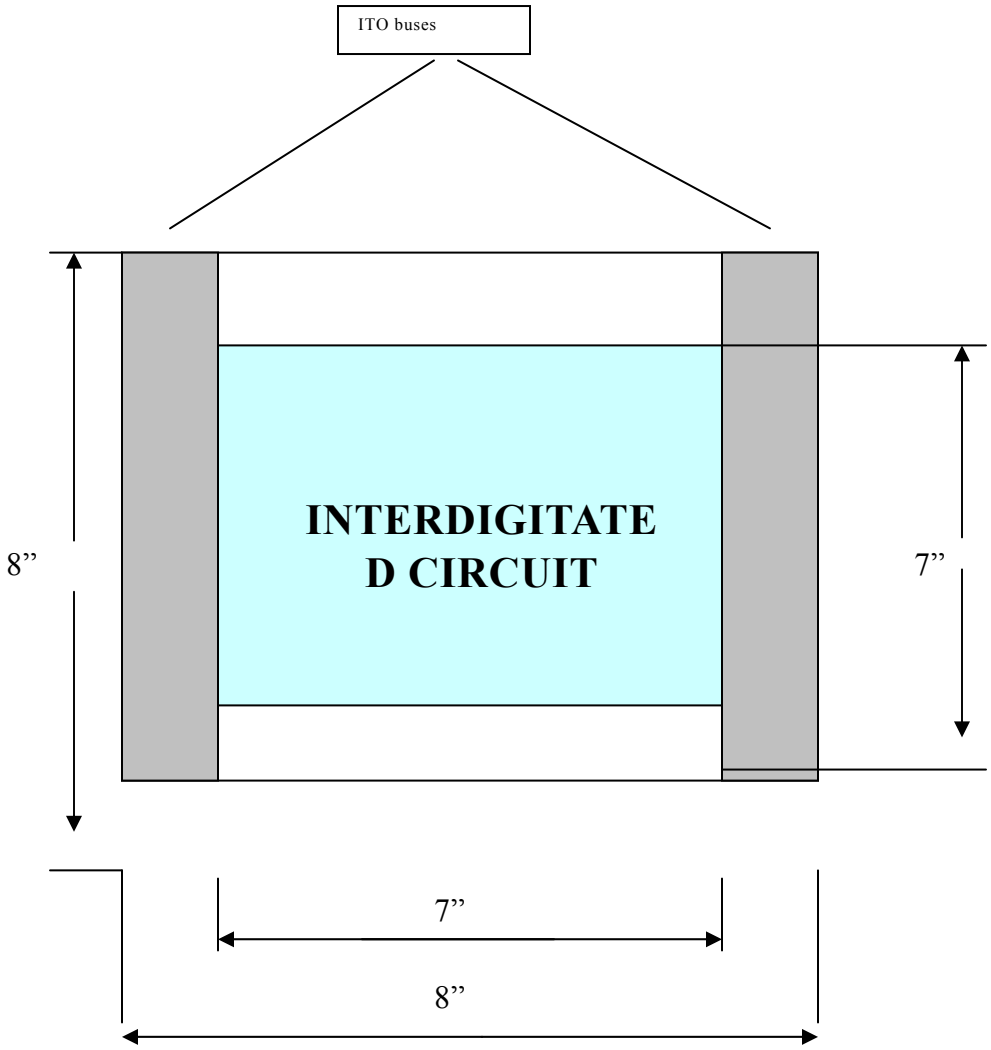

Figure 15. De-icer dimensions

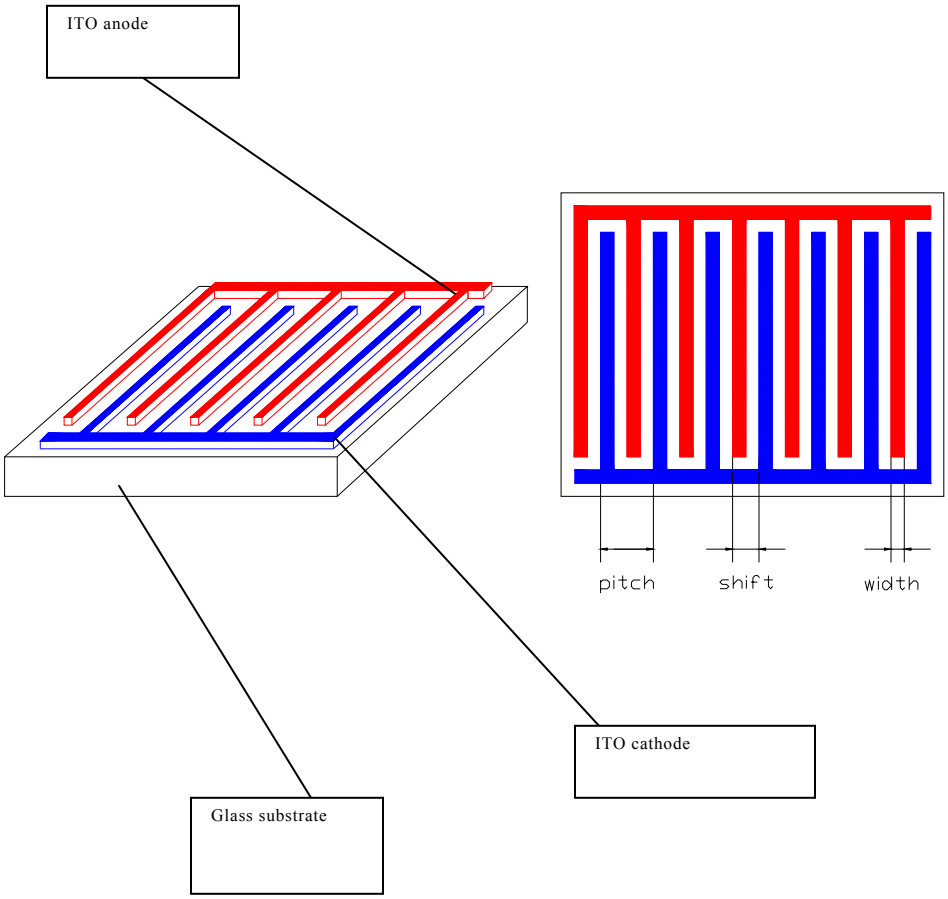

Width = 50 μm;
Shift = 100 μm;
Pitch = 200 μm.

Figure 16 Circuit diagram of the de-icing circuits

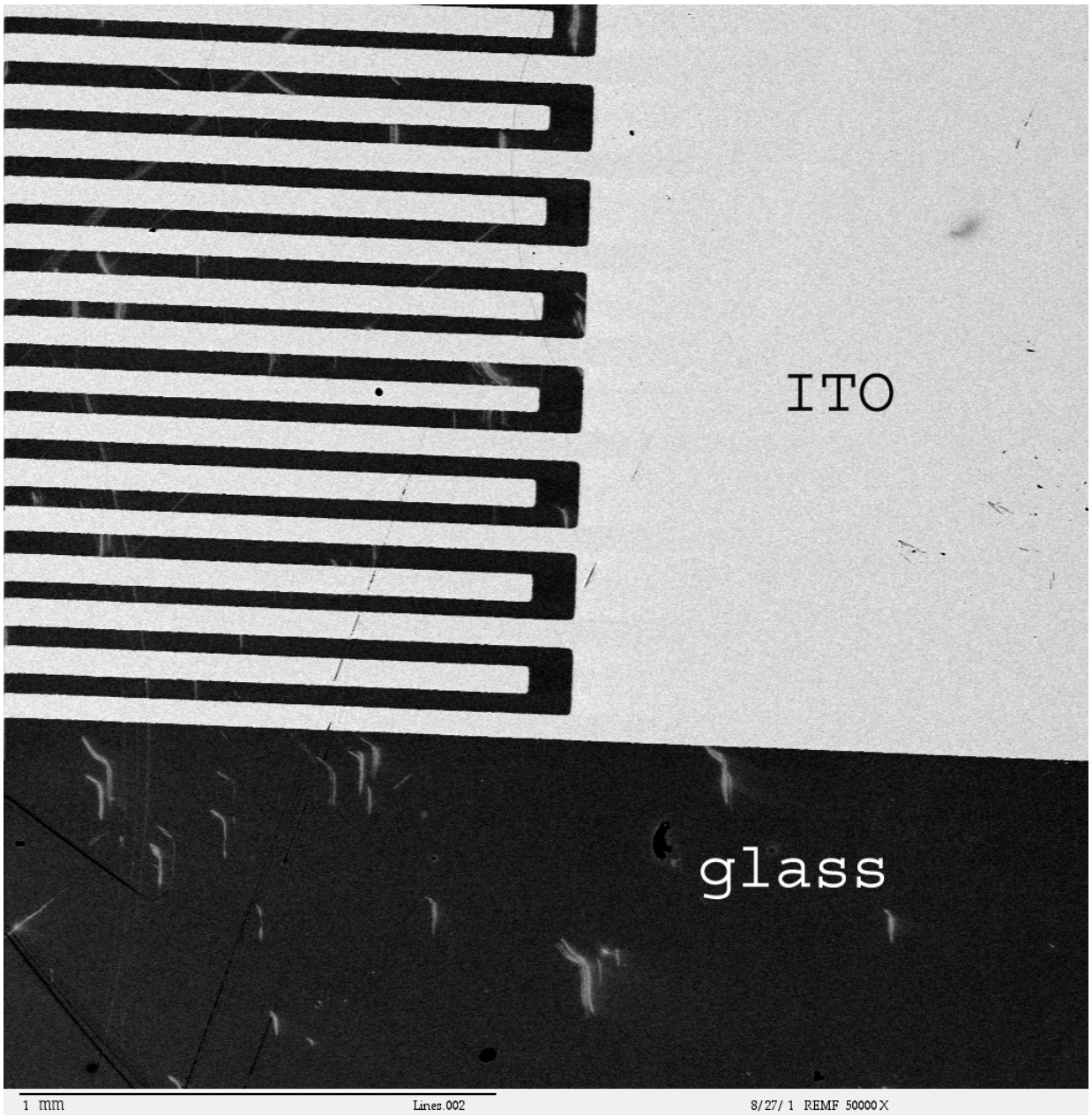

Figure 17. A wide electric bus and narrow electrodes are shown at the edge of the transparent deicer. ITO-coated glass (Compagnie de Saint-Gobain, France), SEM image (Zeiss DSM-962) (Back-Scattered Electron image).

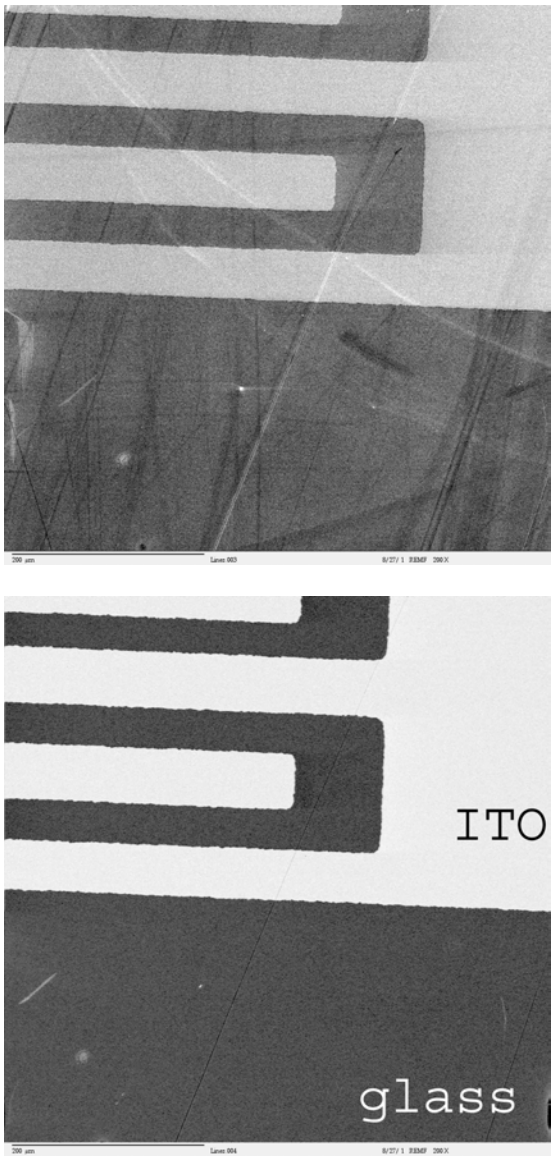

Figures 18, 19. Microstructure of ITO lines (2 is Second Electron Image; 3 is back-scattered Electron image)

The ITO interdigitated circuits were then protected with 4-μm thick layer of SiO2 deposited with Sol-Jel technology.

We have recently designed and successfully manufactured with help from a third party ten 7" x7" transparent HF-deicers. The de-icers were made using 8-ohm/□ ITO of over 90% light transmittance. For protection of ITO circuits they were then coated with 1-micron of SiO2. The circuits have 300-μm lines and 500-μm period.

The theory of HF-deicers has been developed and available now for deicer optimization. Some unexpected theoretical result is that to increase de-icer performance one has to increase the electrodes' width for the expense of higher voltage. Then, a short

pulse of high-power will make ice jumping off the windshield. Thus, in a mode typical for starting a car motor with a starter the windshield can be de-iced in few seconds. Then keeping a very low power we can keep the windshield free of ice. That theoretical prediction has been successfully tested with metal electrodes and is waiting for a windshield test. Use of larger electrodes (up to 1-mm wide) makes photolithography obsolete. We now can use much cheaper technology such as screen-printing and ink-jet printing. Using ink-jet printing we will make soon the circuits on glass by printing with transparent conductive polymers.

3.7.3 Icing research wind tunnel

Design and assembling of a new icing wind tunnel at Dartmouth College.

Development of new type de-icers take numerous wind-tunnel tests.

Figure 20. The icing wind tunnel in a cold room.

We found and purchased a used research wind tunnel and upgraded the tunnel making it an icing one. The modifications and upgrading included installation of laminators of air

flow, reverse of motor rotation direction and installation of a different ventilator, installation of a water spray, design and installation of heaters for water and air lines, design and installation of a share-stress tester. The wind tunnel can operate in a temperature range from 0°C to -45°C. Maximum air speed is 146 km/h inside the 20 cmx20 cm working part of the tunnel, water content can vary from 0.1 to 1 g/m3 providing growth rate of ice from about 0.25 mm/min to 2.5 mm/min.

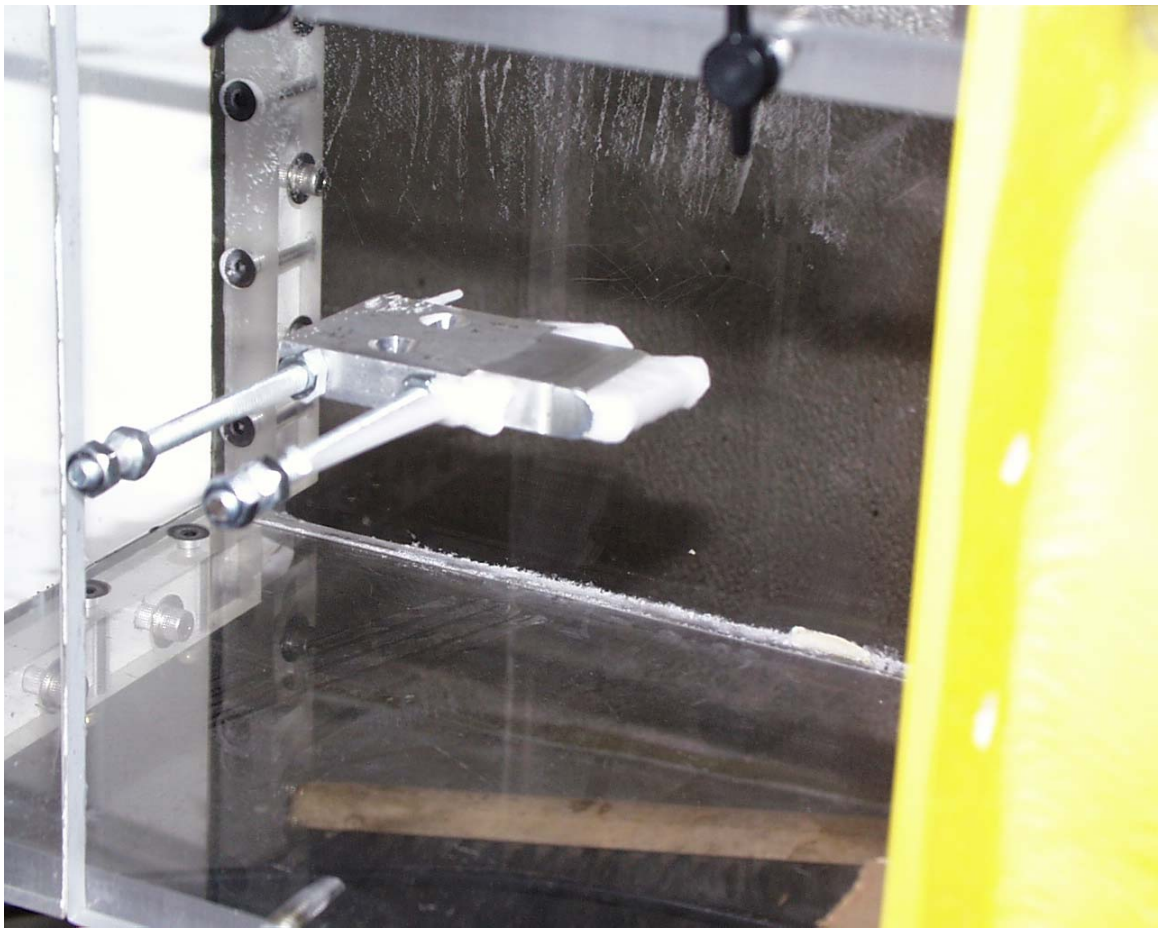

Figure 21. Atmospheric ice growing in the wind tunnel on the aluminum sample. T=-12°C, v=70 km/h, water content =0.5 g/m3.

3.7.4 Some results of de-icing tests results obtained in the wind-tunnel.

The samples were tested in the IWT of Thayer School of Engineering. The samples were tested in a temperature range of -5°C to -30°C, at air speed from 35 km/h to 75 km/h, and with water content in air from 0.2 g/m3 to 1 g/m3.

We found that at power level of about 1kw/m2 it takes less then one minute for gas bubbles to grow over the sample area and to break ice. At even higher power levels a strong water

steam flow is seen coming from the interface and ice can even jump-off the glass. Dependence of ice interfacial strength on power below 1kw/m2 is shown in figure 22. Shot movies demonstrating de-icing action of a similar interdigitated circuits on transparent Kapton can be seen in Appendix II.

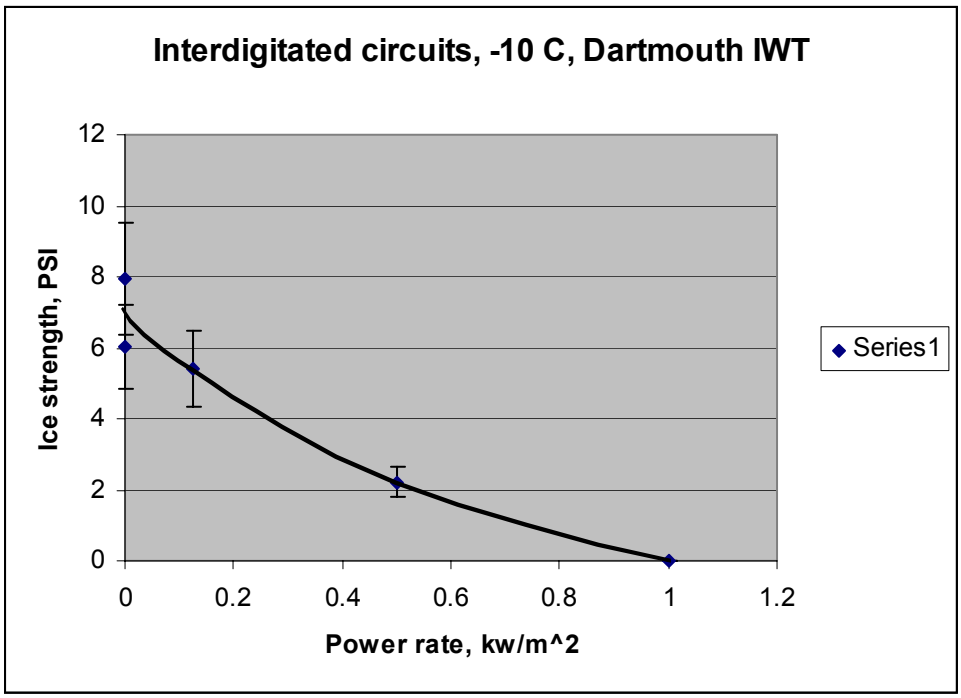

Figure 22. Strength of ice grown on interdigitated circuits as a function of power rate. -10°C, 70 km/h air speed, 0.75g/m water content.

To compare the effect of HF de-icers with the effect of conventional DC –heaters we replaced in several tests our circuits with mesh-based DC-heaters. These important tests didn't reveal any obvious effect of electric heating on ice strength in the wind of 75 km/h when we applied the same power as in the cases of various meshes and interdigitated circuits. It means, that what HF power does to ice is not a simple heating. It is known in the industry that it takes much higher power rate to de-ice aerofoils with conventional heaters. It typically takes from 30 to 45 kw/m2 as compared with ≤ 1kw/m2 required for HF-de-icer. On a resting car 200 to 300w/m2 will be enough for efficient de-icing.

3.7.5 HF-airplane de-icer

In the past we have developed and manufactured several types of ice-electrolysis de-icers. The de-icers were then tested in cold rooms and the ASD Icing Wind Tunnel. Though, in many tests some de-icers demonstrated outstanding performance, including spontaneous cleaning of aerofoils, the tests also revealed a serious technological challenge. Namely, it was extremely difficult to make grids of electrodes that could satisfy several

requirements: infinite resistance to electro corrosion, strong adhesion in between all the components that can withstand action of ice and water electrolysis, and very small dimensions of electrodes and inter-electrode space. To overcome these problems we invented and theoretically developed a new de-icer that uses HF-dielectric heating principle. The background of the new method was described in detail above. In the year 2001 we have made and tested in our new icing wind tunnel and in ASD wind tunnel a wide variety of de-icers: woven composite meshes, interdigitated electrodes, plane SS meshes on anodized aluminum, and conventional DC-heaters. Variables in the tests were temperature, wind velocity, water content in air, and the de-icers' dimensions and design. These tests first had to examine efficiency of the new method in comparison with the conventional DC-heating, and in comparison with the electrolysis method. We have also developed new theoretical concepts of HF-de-icers. Several new technologies-experiments have been started and are in current progress. All together that enables us to develop soon much larger and more efficient and robust HF-de-icers for airplanes. That work was performed in collaboration with and

3.7.6. HF-road de-icer

Icing of bridges, sidewalks, airport runways, and other road structures in cold environments is a persistent problem worldwide. The roadway icing can be caused by freezing rain and by melting and refreezing of falling snow. Not only can these types of icing conditions cause delays and slowdown of traffic, but they can also produce dangerous driving conditions. Conventional methods of road de-icing include use of sand and salt, and spray of other environmentally aggressive solutions such as a solution of magnesium chloride. Those chemicals cause corrosion of cars and they also damage metal parts of road structures.

To address that problem Dartmouth College and ARS started in April 2001 a development of a new type of road de-icing system that uses electrochemical decomposition (electrolysis) on ice that is attached to an electrically conductive surface. The work includes the development and testing of several active road de-icers suitable for a bridges, roads, runways, sidewalks, etc., with subsequent international commercialization. In particular, we are: 1) testing candidate materials for use as anodes and cathodes and selecting a dielectric material for use on roadways; 2) Establishing the appropriate requirements for de-icer performance, power requirement, conductivity, electric strength, and mechanical durability; 3) Testing resistance of the coating components to electro corrosion; 4) Designing the coating configuration, and 5) Testing of de-icing and anti-icing performance of the coatings.

A very large volume of research and development work was done during the first half year of the project. Namely:

1. We have developed and tested numerous materials and components of future road de-icers that can withstand the abrasive and corrosive action of aggressive road environment.
2. We have invented, developed and tested several small-size road de-icers with electrolysis action. Thus, the concept of their use was proved. Nevertheless, we are concerned that expensive materials and technologies used in the manufacturing of such de-icers would hardly make them commercially-efficient in road applications.
3. Instead of electrolysis-based de-icing, we invented a new revolutionary method: HF-dielectric heat de-icing. The method showed performance that out-performed that of the electrolysis method. Moreover, HF-de-icers can be built with cheap and durable materials. We are now considering the HF-method for use on roads.
4. The work performed so far completely covers all planned small-scale development.

3.7.7 Effect of HF-electric fields on growth of atmospheric ice

We have observed a total suppression of growth of atmospheric ice on cooled metal surfaces when HF- high strength electric fields have been applied. The metal surfaces have remained well below ice melting point and their temperature has not been affected by the heating power of electric fields.

In the experiment schematically shown in figure 15 an anodized aluminum mesh was used to generate HF-high-strength electric field. Aluminum wires of the mesh were anodized to separate the wires electrically. All the wires running in one direction then were connected to one electric bus while all the wires running in the perpendicular direction were connected to the second bus of a HF-generator, see figure 24.

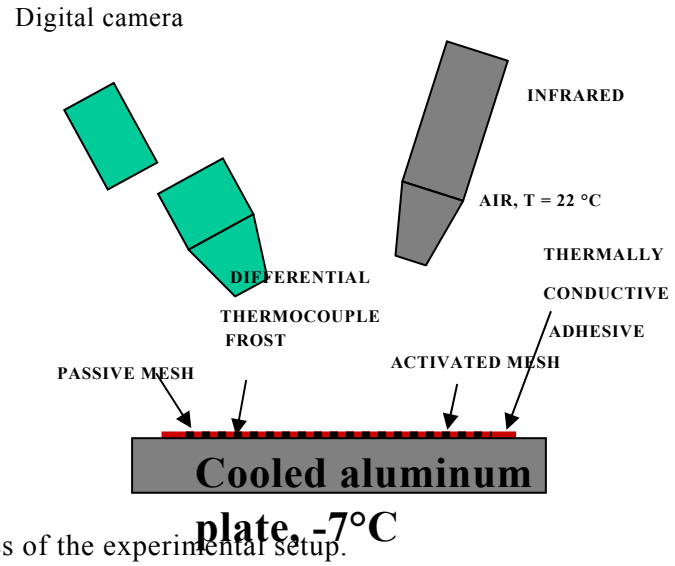

Figure 23. Schematics of the experimental setup.

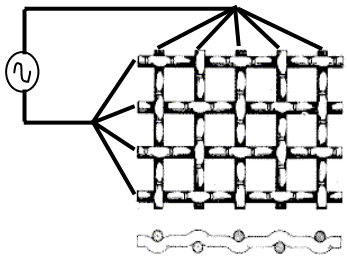

Figure 24. Anodized aluminum mesh 120 (120 wires per inch).

The mesh was attached with thermally conductive adhesive to a cold plate kept at -7°C inside a warm room. To increase humidity a flux of water mist from an air humidifier was directed to the mesh. The mesh temperature was controlled with two thermocouples attached directly to the mesh and also with a remote infrared optical thermometer.

Only one-half of the mesh was connected to a HF-power supply. 20 kHz voltage of 35-volts rms has been applied to the activated part of the mesh. The corresponding power consumption rate has not exceeded 4 watt/m^2 during that experiment and the HF-power has not affected the mesh temperature within our accuracy of measurements (±0.25°C). Nevertheless, we have observed a very drastic difference in icing of the "activated" and the “passive” parts of the mesh, see figure 4. The activated mesh remained cleaned of ice and frost all the time while we observed rapid growth of frost and ice on the passive half of the mesh. A sharp boundary between the two regions can be seen in figure 25. A mean strength of the electric field in that experiment was 2.8 kV/cm.

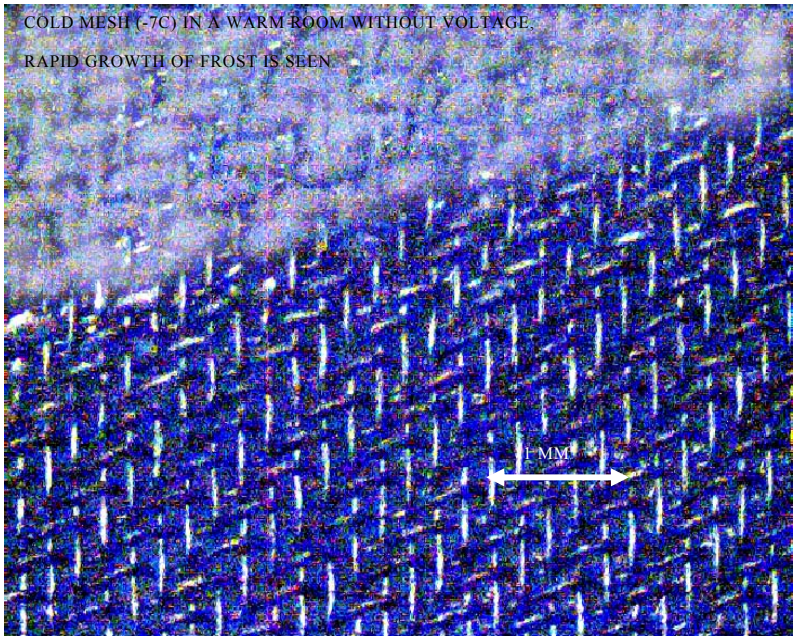

Figure 25.1Microscopic image of a sharp boundary between the activated and non-activated aluminum meshes.

We will study in more detail this new physical phenomenon to uncover its physical mechanism.

3.7.8 *In situ* study of atmospheric ice

As it was discussed at ARO Ice and Snow Strategic Workshop (March 2001, Hanover, NH) physical properties of growing atmospheric ice at a given temperature may differ from solid ice at the same temperature. The reason for that difference is unfrozen water in pours and channels. Due to very large difference in electrical properties of water and ice we decided to measure *in situ* conductivity and dielectric permittivity of ice growing from water spray in an icing wind tunnel. We have also examined thin cross sections of the ice for any evidence of unfrozen water.

The ice samples were grown under experimental conditions shown in the table below. Figure 18 shows the grown ice sample. Thin section of the ice were cut from the central part of ice samples along AA'-line. The sections were then examined in a microscope through two optical cross-polarizers. Examples of such cross sections are shown in figures 27-29. The structure and density of air-filled pours was different for ice grown on the stagnation line and on the inclined parts of the aerofoils.

3.7.9 Test conditions for making thin sections of ice.

Run no.	Mesh size	Temp. (C)	Wind speed (km/h)	Water rate (ml/min.)	Duration (min.)
110501	50mesh	-10	75	35-40	10
110703	50mesh	-9.7	75	35-40	10

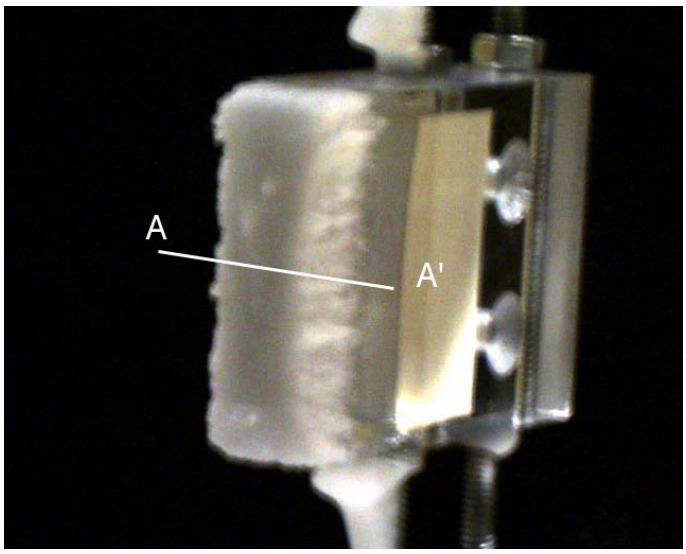

Figure 26. Ice sample on 50mesh on a 1"-thick sample holder (#110703).

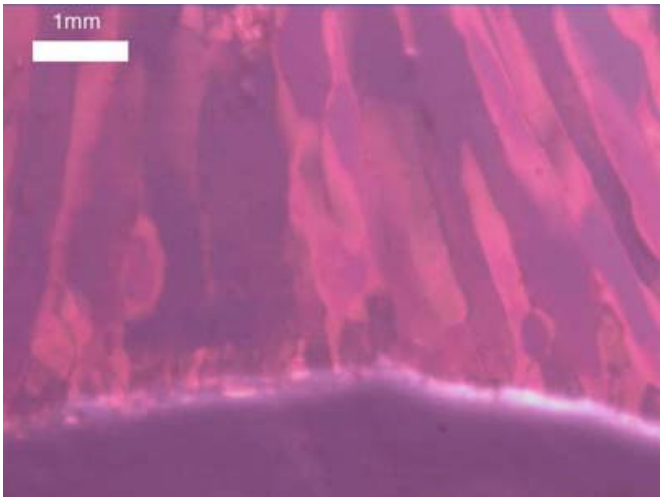

Figure 27. Thin section of the center part (#110703).

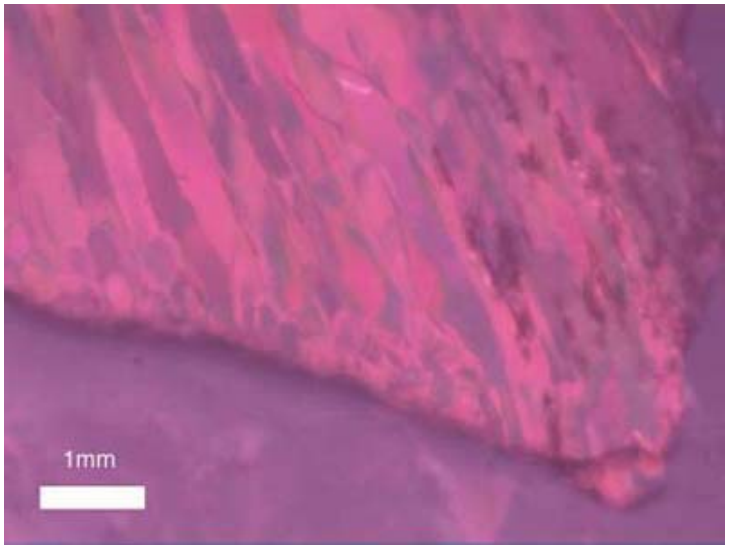

Figure 28. Thin section of a side part (#110703). Black lines at the right side of the picture correspond to white area of ice sample in Fig 18.

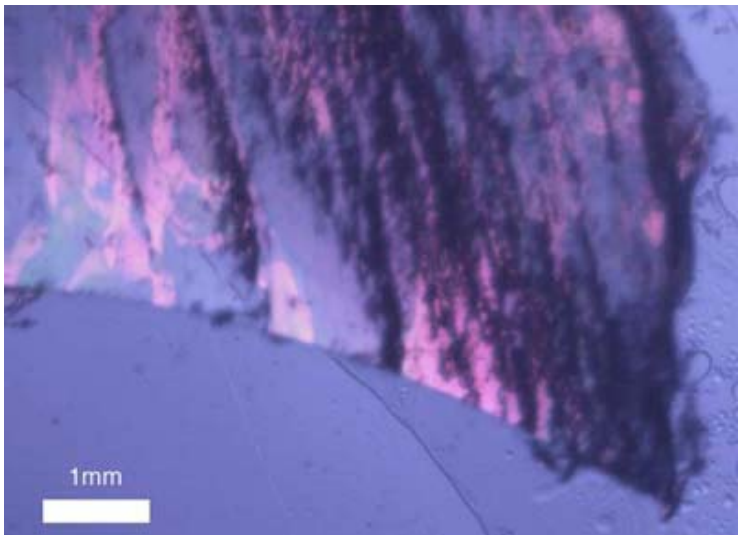

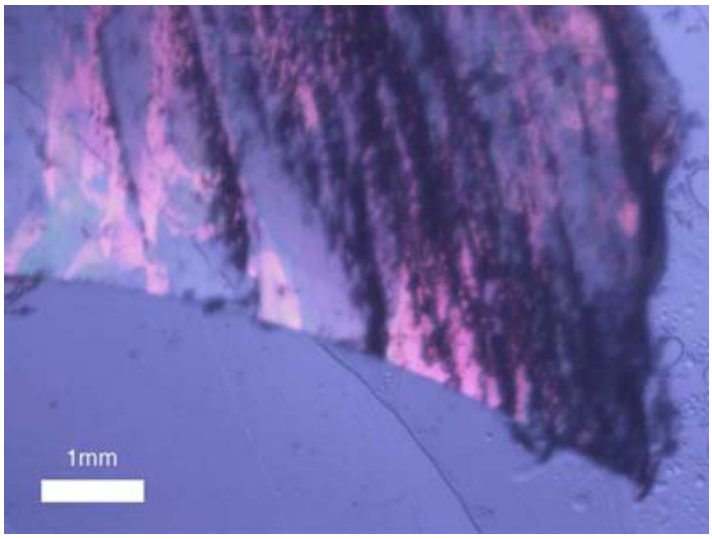

Figure 29. Thin section of side part (#110501). It was thicker than #110703 so that black lines at the right side of the picture can be observed clearly.

To measure *in situ* the conductance and capacitance of ice a HP low-frequency impedance analyzer was used. The measurements were performed at temperatures of –9 C and –20 C, at air speed of 75 km/h, and with water-supply rate of 20 ml/min. The table below shows the tests conditions. Mesh electrodes were used in these experiments. We applied a chemical tape with small windows to measure ice conductivity at different locations, see figures 30-31.

Figures 30-31 show time-dependence of the conductance and the capacitance of ice. Experimental conditions and some preliminary results of the in situ measurements of the conductance and the capacitance of ice in Thayer School WT at 20kHz are shown in the table below.

Run no.	**Temp. (C)**	**Wind speed (km/h)**	**Water rate (ml/min.)**	**Location**	**Open surface (cm^2)**	**Max. Conductance (μS)**	**Max. Capacitance (nF)**
111202	-9.6	75	20	whole	17.16	239	5.28
111302	-8.6	75	21	side	1.00	27.5	2.31
111303	-8.4	75	21	center	1.00	17.7	2.24
111602	-20.3	75	20	center	1.00	6.6	1.979
111604	-20.4	75	23	center	1.00	8.5	1.993
111605	-20.5	75	18	side	1.00	11.6	2.11

As seen from the table and also from figures 32-33 the conductivity and dielectric constant of ice passes several stages reflecting ice/water changes in ice thickness and water content inside the ice.

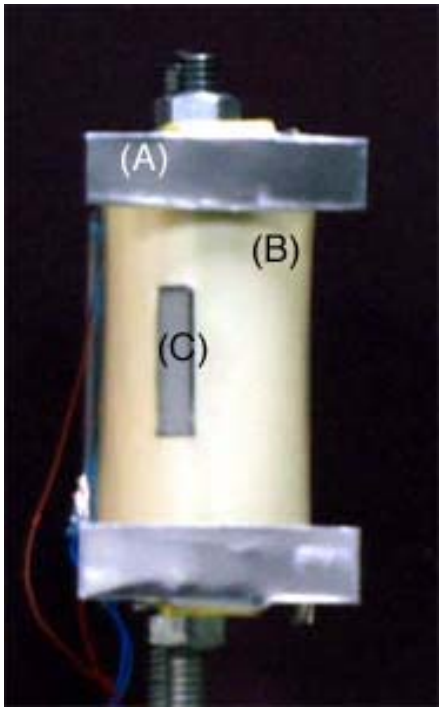

Figure 30. Mesh sample with a chemical tape and a hole on a side. Opening size is 0.5cm x 2 cm. (A) Screens, (B) Chemical tape, (C) Opening.

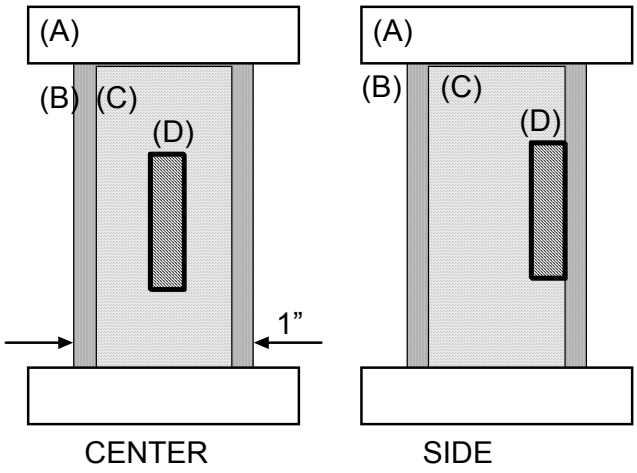

Figure 31. Schematic drawing of the measuring positions. Center position (left) and Side position (right). The side position is almost on the edge of ice. (A) Screens, (B) Chemical tape, (C) Ice sample, (D) Opening.

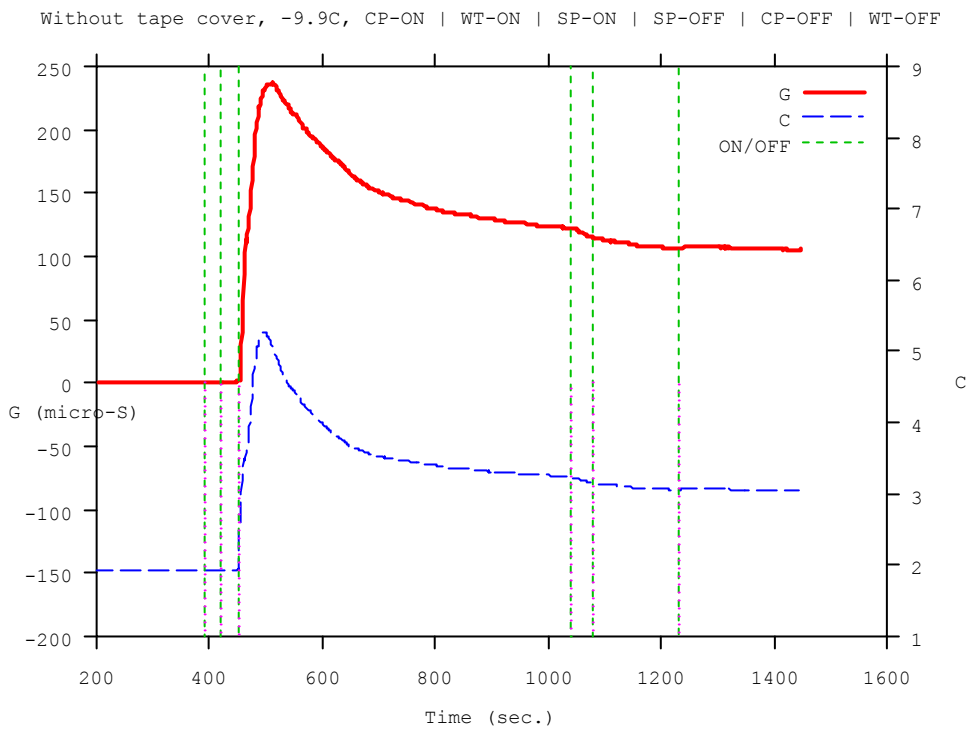

Figure 32. History of the conductance and the capacitance of ice. #111202. G: Conductance, C: Capacitance. The lines show time when the wind was turned on and off. The double-dashed lines show when the water-spray was turned on and off.

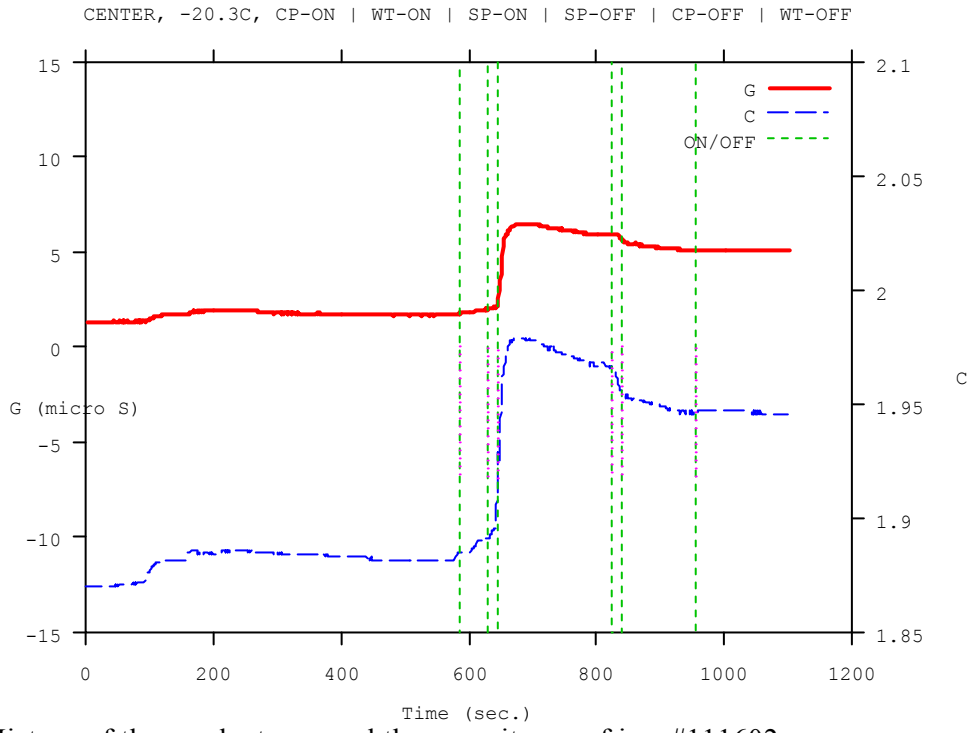

Figure 33. History of the conductance and the capacitance of ice. #111602.

We are planning to continue these very important experiments in near future.

3.7.10 Theory of ice surface structure

A new theoretical model of a quasi-liquid layer on the ice surface was proposed. The model is based on the recently developed theory of the transition of ice into a Bernal-Fowler state. The model does not need any additional assumption and it's capable to explain the unique properties of ice surface that arise from a reduction in the lattice order parameter due to the specific boundary condition on the ice surface. The theory may be directly generalized to the ice/solid interfaces.

4. Collaboration and partnership with industry.

During years 1999-2003 we have deepened and expended collaboration with several US companies:

1. Goodrich Corporation was our largest industrial partner. We are currently working together on a HF-de-icer for aerospace applications. We have also discussing a partnership with Goodrich in development of a power-line de-icer. Goodrich is also interested in a new license for de-icing of wind-mill power stations.
2. Advanced Recycling Sciences is our licensee and a partner in the development of a road de-icer.
3. Torvec Inc. is our licensee and a partner in the development of a car windshield de-icer and electrostatic ice breaker.
4. New York Power Authority is our partner in development of power-line de-icers.
5. We have been and are in contacts/discussions on future joint projects with about a dozen of national and international companies such as Sumitomo-Dunlop (Japan), Continental Tire (Germany), Guardian Glass Industries, PPG Co., Bird Air Co., Burton Co., Karhu Inc., Five-Ten Inc., and others.